Supplementary Materials for

Ferroelectric α-Bi_2O_3 films derived from β-Bi via ultraviolet ozone oxidation

Wei Li[1,2], Wei Zhang[1*], Lingyuan Kong[1,2], Tianci Hu[2], Zeguo Lin[2], Yi Jiang[2], Fang Yang[2], Yang Guo[2], Pan Chen[2], Runzhang Xu[3*], Yan Liang[2*] and Jiandi Zhang[2,4*]

[1]*Hebei Key Lab of Optic-electronic Information and Materials, College of Physics Science and Technology, Hebei University, Baoding 071002, China.*

[2]*Beijing National Laboratory for Condensed Matter Physics, Institute of Physics, Chinese Academy of Sciences, Beijing 100190, China.*

[3]*Department of Physics, The Hong Kong University of Science and Technology, Hong Kong 999077, China.*

[4]*College of Physics, University of Chinese Academy of Sciences, Beijing, 100190, China.*

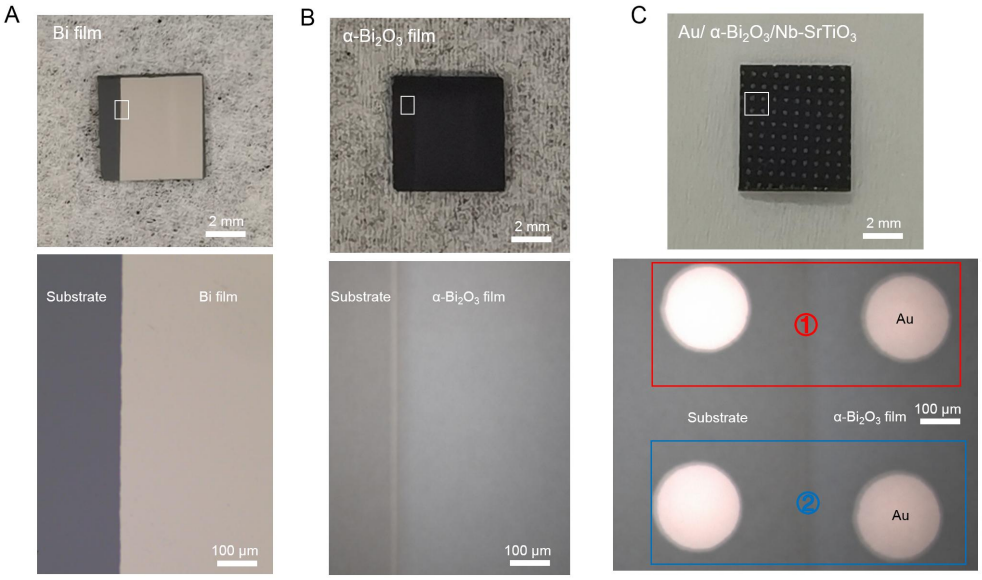

Fig. S1 Macroscopic photographs and optical microscopy images of the samples and devices. (A) Macroscopic photograph and optical microscopy image of the precursor Bi film before oxidation.(B) Macroscopic photograph and optical microscopy image of the α-Bi_2O_3 film after oxidation.(C) Macroscopic photograph and optical microscopy

image of the fabricated Au/α-Bi_2O_3/ Nb-$SrTiO_3$ vertical devices. The circular regions correspond to the Au top electrodes. The red and blue boxes mark two representative device groups.

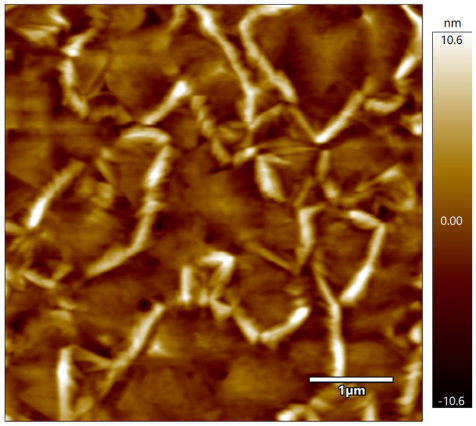

Fig. S2 AFM image of the α-Bi_2O_3 film.

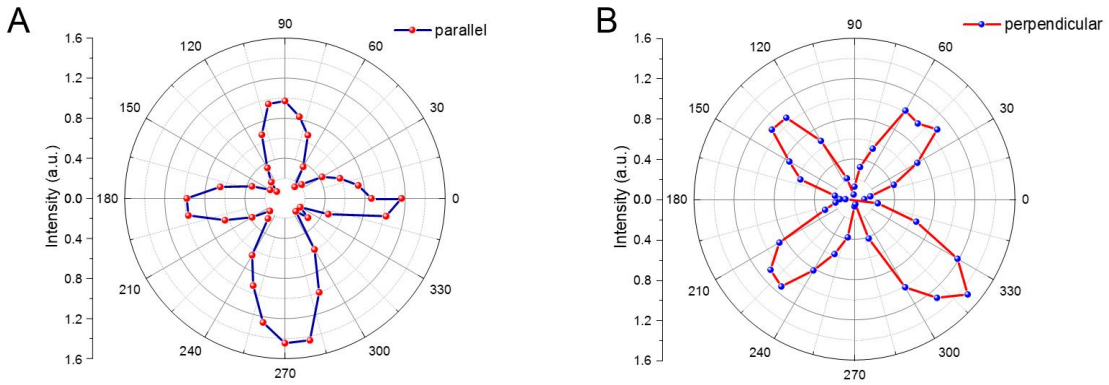

Fig. S3 Polarization-dependent SHG measurements of α-Bi_2O_3 films. Angular dependence of the SHG intensity under out-of-plane excitation for (A) parallel and (B) perpendicular polarization configurations. The nonzero SHG signals and characteristic rotational anisotropy patterns provide evidence for broken inversion symmetry in the ultrathin α-Bi_2O_3 films.

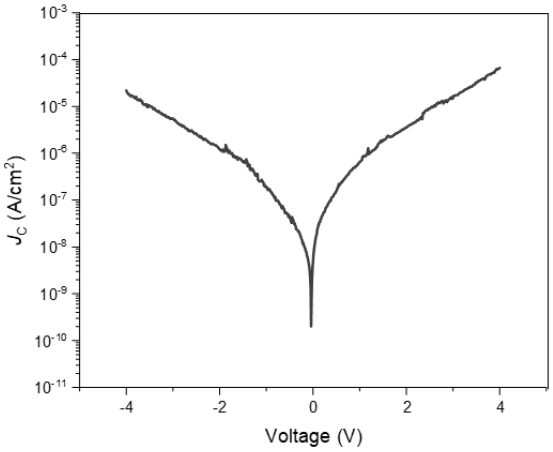

Fig. S4 Room-temperature leakage current density of the Au/α-Bi_2O_3/Nb-$SrTiO_3$ capacitor structure.

Table. S1 Comparison of ferroelectric properties of α-Bi_2O_3 and representative Bi-based ferroelectric materials, including their crystal structures, film thicknesses, and polarization characteristics.

Materials	Structure	Thickness	Polarization
Bi_2WO_6[1], [2]	layered perovskite	ultrathin film	in-plane (~50 μC/cm^2)
$SrBi_2Ta_2O_9$[3]	layered perovskite	thin film	in-plane (~10 μC/cm^2)
$Bi_4Ti_3O_{12}$[4]	layered perovskite	bulk	in-plane (~8 μC/cm^2)
Bi_2AlMnO_6[5]	double perovskite	thin film	out-of-plane (--------)
Bi_2NiMnO_6[6]	double perovskite	thin film	out-of-plane (~5 μC/cm^2)
Bi_2O_2Se[7]	two dimensional layered	ultrathin film	out-of-plane (~35 μC/cm^2)
BiCuSeO[8]	two dimensional layered	ultrathin film	out-of-plane (--------)
Bi_2TeO_5[9]	two dimensional layered	ultrathin film	in-plane (~5 μC/cm^2)
α-Bi_2SeO_5[10]	two dimensional layered	ultrathin film	out-of-plane (~22 μC/cm^2)
Sm doped Bi_2O_3[11]	layered oxide	ultrathin film	out-of-plane (~50 μC/cm^2)
α-Bi_2O_3 (this work)	binary oxide	ultrathin film	out-of-plane (~6 μC/cm^2)

[1] Zhou, S.; Liao, L.; Chen, L.; Feng, B.; He, X.; Bai, X.; Song, C.; Wu, K. Ferroelectricity in Epitaxial Perovskite Oxide Bi_2WO_6 Films with One-Unit-Cell Thickness. *Nano Lett.* **2023**, 23 (17), 7838–7844.

[2] Jeong, J.; Mun, J.; Das, S.; Kim, J.; Kim, J. R.; Peng, W.; Kim, M.; Noh, T. W. Growth and Atomically Resolved Polarization Mapping of Ferroelectric Bi_2WO_6 Thin Films. *ACS Appl. Electron. Mater.* **2021**, 3 (2), 1023–1030.

[3] Lee, E.; Son, J. Y. Growth and Ferroelectric Properties of $SrBi_2Ta_2O_9$ Thin Films on Highly Oriented Pyrolytic Graphite Substrates with Atomic Structure like Graphene Surface. *J. Mater. Sci.* **2024**, 59 (32), 15399–15407.

[4] Long, C.; Chang, Q.; Fan, H. Differences in Nature of Electrical Conductions among $Bi_4Ti_3O_{12}$-Based Ferroelectric Polycrystalline Ceramics. *Sci. Rep.* **2017**, 7 (1), 4193.

[5] Li, L.; Boullay, P.; Lu, P.; Wang, X.; Jian, J.; Huang, J.; Gao, X.; Misra, S.; Zhang, W.; Perez, O.; Steciuk, G.; Chen, A.; Zhang, X.; Wang, H. Novel Layered Supercell Structure from Bi_2AlMnO_6 for Multifunctionalities. *Nano Lett.* **2017**, 17 (11), 6575–6582.

[6] Zhong, W.-M.; Liu, Q.-X.; Tang, X.-G.; Jiang, Y.-P.; Li, W.-H.; Li, W.-P.; Cheng, T.-D. Ferroelectric Diode Effect with Temperature Stability of Double Perovskite Bi_2NiMnO_6 Thin Films. *Nanomaterials* **2019**, 9 (12), 1783.

[7] Kong, L.; Li, W.; Hu, K.; Fan, Z.; Yin, Z.; Ling, H.; Wang, Z.; Li, D.; Tai, S.; Li, C.; Jabeen, F.; Guo, Y.; Xu, R.; Yang, F.; Guo, J.; Zhang, W.; Chen, P.; Liang, Y.; Zhang, J. Room-Temperature Ferroelectricity of Bi_2O_2Se in the Two-Dimensional Limit. *Nano Lett.* **2025**, acs.nanolett.5c04402.

[8] Kong, L.; Li, W.; Wang, Z.; Fan, Z.; Yin, Z.; Ling, H.; Hu, K.; Tai, S.; Li, D.; Li, C.; Guo, Y.; Yang, F.; Zhang, W.; Guo, J.; Xu, R.; Chen, P.; Liang, Y.; Zhang, J. Room-Temperature Ferroelectricity in Ultra-Thin p-Type BiCuSeO Films. ***Adv. Mater.*** **2025**, 37 (45), e10566.

[9] Han, M.; Wang, C.; Niu, K.; Yang, Q.; Wang, C.; Zhang, X.; Dai, J.; Wang, Y.; Ma, X.; Wang, J.; Kang, L.; Ji, W.; Lin, J. Continuously Tunable Ferroelectric Domain Width down to the Single-Atomic Limit in Bismuth Tellurite. *Nat. Commun.* **2022**, 13 (1), 5903.

[10] Wu, Q.; Li, Z.; Han, B.; Sun, W.; Liu, Q.; Xue, C.; Bae, H.; Wang, M.; Fu, B.; Qian, J.; Zhu, Y.; Sun, Y.; Feng, T.; Gao, X.; Cong, X.; Liu, W.; Gao, Y.; Yan, B.; Tan, C.; Liu, H.; Peng, H. Wafer-Scale Ultrathin and Uniform van Der Waals Ferroelectric Oxide. *Science* **2026**, 391 (6784), eadz1655.

[11] Yang, Q.; Hu, J.; Fang, Y.-W.; Jia, Y.; Yang, R.; Deng, S.; Lu, Y.; Dieguez, O.; Fan, L.; Zheng, D.; Zhang, X.; Dong, Y.; Luo, Z.; Wang, Z.; Wang, H.; Sui, M.; Xing, X.; Chen, J.; Tian, J.; Zhang, L. Ferroelectricity in Layered Bismuth Oxide down to 1 Nanometer. *Science* **2023**, 379 (6638), 1218–1224.